

# New Short-Circuited Coaxial Method Implementation for Complex Permittivity Measurement of Power Transformer Oils

Ahmad Abualasal<sup>1\*</sup>, István Kiss<sup>1</sup>

<sup>1</sup> Department of Electric Power Engineering, Faculty of Electrical Engineering and Informatics, Budapest University of Technology and Economics, H-1521 Budapest, P.O.B. 91, Hungary

\* Corresponding author, e-mail: [ahmadabualasal@edu.bme.hu](mailto:ahmadabualasal@edu.bme.hu)

Received: 24 June 2023, Accepted: 12 April 2024, Published online: 18 June 2024

## Abstract

The investigation into the dielectric properties of transformer oils has been a focal point in both historical and contemporary electric insulation technology as high-voltage applications have greatly benefited from the continuous research efforts in this field. The dielectric permittivity is one of the factors to be negotiated when discussing the electric insulation of any material. This work aims to showcase a new short-circuited coaxial cable method to evaluate the complex dielectric permittivity of palm, sunflower and rapeseed oil and review other previously used measurement techniques. Mainly, the test was performed using a sample holder that represents a short-ended coaxial cable filled with the test material which is connected to one port of a vector network analyser. The measurements of the input impedance for various oil samples were conducted at frequencies ranging from 1 MHz to 10 MHz. The technique uses the value of the input impedance which depends on the reflected signals from the test sample to the network analyser, consequently, the value of the dielectric permittivity and dielectric loss have been calculated using the short circuit impedance formula which involves numerical methods to get the results which shows that this method can be used as an alternative to investigate the oils insulation parameters as it provides smooth results for permittivity without any divergence, ensuring more reliable and consistent measurements as well as providing high accuracy in determining the permittivity of materials.

## Keywords

insulation, dielectric permittivity, coaxial cable, transmission/reflection, short-circuit line

## 1 Introduction

Power transformers play a major role in the functioning and stability of electrical grids worldwide. Serving as indispensable components, these transformers facilitate the efficient transmission and distribution of electricity across various voltage levels within the grid infrastructure. By stepping up voltage levels for long-distance transmission and stepping down voltage levels for local distribution, power transformers enable electricity to be transported economically over vast distances with minimal losses. Furthermore, they provide voltage regulation, impedance matching, and isolation, ensuring that electricity reaches consumers reliably and safely. Given their critical function in the grid, the reliability, performance, and longevity of power transformers are paramount for maintaining the integrity and resilience of the entire electrical infrastructure. The dielectric permittivity of insulating materials in power transformers is crucial for maintaining insulation integrity, preventing electrical breakdown, and

ensuring efficient energy transmission. It directly impacts factors like insulation strength, capacitance, and energy losses within the transformer. Optimizing dielectric permittivity is essential for designing reliable transformers that meet stringent performance and safety standards, thus contributing to grid stability and resilience. Particularly in the scientific areas of material science, microwave circuit design, absorber development, biological research, etc., the measurement of the dielectric characteristics of materials at radio frequency has grown in significance. Dielectric measurement is crucial because it can reveal a material's electrical or magnetic properties, which have been helpful in numerous research and development domains. To measure these intricate features, numerous techniques, including those in the time domain or frequency domain with one port or two ports, have been devised. Every technique has limitations due to the materials, frequencies, and applications that it can use. With the development of new

technologies, the techniques can be used with software that runs a vector network analyser to measure the complex reflection and transmission coefficients and convert the data into the complex dielectric property parameter [1, 2].

The complex relative permittivity ( $\epsilon_r$ ) of the materials is measured in order to determine the dielectric characteristics. There are two parts to a complex dielectric permittivity: a real part and an imaginary part. The quantity of energy from an external electrical field that is stored in the material is indicated by the real part of the complex permittivity, also referred to as the dielectric constant. The imaginary component, commonly referred to as the loss factor, is zero for lossless materials. It is a gauge of how much energy a material loses to an outside electric field. The ratio of the complex permittivity's imaginary to real parts is represented by the term ' $\tan \delta$ ', often known as the loss tangent [3].

## 2 Methods

### 2.1 Transmission/reflection line method

The Transmission/Reflection line method requires putting a sample in a section of waveguide or coaxial line and using a vector network analyser (VNA) to measure the two ports' complicated scattering properties as illustrated in Fig. 1. Prior to taking the measurement, calibration must be done. Intercomparison of Permittivity Measurements Using the Transmission/reflection Method in 7-mm Coaxial Transmission Lines [4].

The process entails measuring the transmitted signal ( $S_{11}$ ) and reflected signal ( $S_{21}$ ). In the VNA,  $S_{11}$  and  $S_{21}$  are key parameters that characterize the behaviour of the

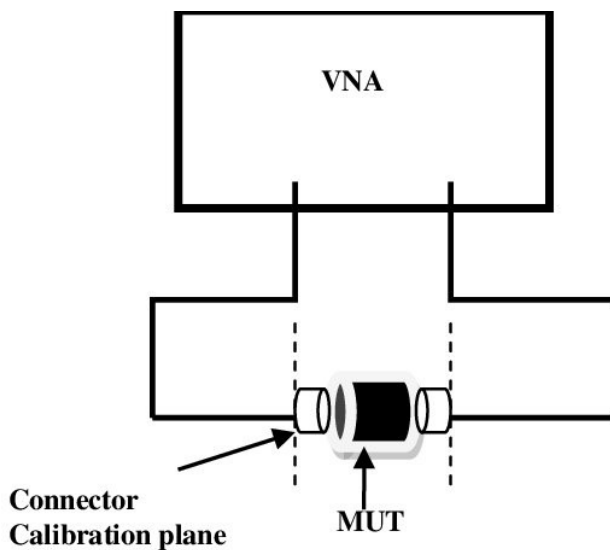


Fig. 1 The TR method waveguide implementation

material under test (MUT) or the device under test (DUT), typically a two-port network or component, such as a transmission line, amplifier, or filter.

$S_{11}$  parameter represents the reflection coefficient of the DUT at Port 1. It quantifies the amount of signal reflected back towards the input of the device, indicating how well the device impedance matches the characteristic impedance of the connected transmission line or system. Consequently,  $S_{21}$  parameter represents the transmission coefficient from Port 1 to Port 2. It quantifies the amount of signal transmitted from the input of the device to the output, providing information about the insertion loss or gain of the device.

The complex permittivity and permeability of the material are tightly related to the pertinent scattering characteristics by the following equations:

$$S_{11} = R_1^2 \left[ \frac{(1-z^2)}{1-\Gamma^2 z^2} \Gamma \right] \quad (1)$$

$$S_{22} = R_2^2 \left[ \frac{(1-z^2)}{1-\Gamma^2 z^2} \Gamma \right] \quad (2)$$

$$S_{12,21} = R_1 R_2 \left[ \frac{(1-\Gamma^2)}{1-\Gamma^2 z^2} z \right] \quad (3)$$

Where:

$$R_1 = \exp(-\gamma_0 L_1) \quad (4)$$

$$R_2 = \exp(-\gamma_0 L_2) \quad (5)$$

are the reference plane transformation expressions and  $L_1, L_2$  is the distance between the sample and port 1 and port 2 respectively as illustrated in Fig. 2 where the transmission and reflection coefficients are also denoted. The transmission coefficient is defined by:

$$z = (-\gamma L) \quad (6)$$

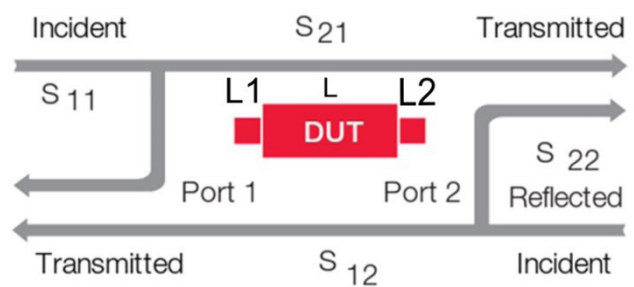


Fig. 2 The scattering parameters implementation around the DUT

L is the length of the sample between the ports, whereas the reflection constant for the sample material ( $\Gamma$ ) which is a function of the propagation constant ( $\gamma$ ) and the permeability ( $\mu$ ) for the material and the same parameters for the vacuum; it can be found using:

$$\Gamma = \frac{\frac{\gamma_o - \gamma}{\mu_o - \mu}}{\frac{\gamma_o + \gamma}{\mu_o + \mu}} \quad (7)$$

By utilizing a program to solve the equations, it is possible to calculate the conversion of s-parameters to complex dielectric parameters. It is frequently necessary to prepare the sample for the procedure, such as by machining it, to make it fit snugly inside the waveguide or coaxial line.

Transmission line calibrations employ a variety of terminations that cause the transmission line to behave in a variety of resonant ways. Maximum electric field, which can be attained through open circuited or other capacitive termination, is necessary for accurate dielectric measurement, whereas calibration in coaxial line measurements can be performed using either short circuited, open circuited, or matched load termination. The measurement technique enables the measurement of the dielectric material's permittivity and permeability [5, 6].

The material under test (MUT) is then set up in a sample holder once the VNA has been calibrated at the connector calibration plane. To minimize the measurement uncertainty brought on by air gaps, the MUT must fit perfectly inside the sample holder [2]. There are two ways to extend the calibration plane to the sample surface. The phase factor, which corresponds to the distance between the sample surface and the connector calibration plane, is manually fed into the system as the first method. With the use of the VNA's features, the phase factor may be simply incorporated into the measurement. The calibration plane will be moved by the VNA from the connector to the MUT surface [7].

After calibration is complete, the method requires measuring the s-parameter of an empty sample holder. The network analyser is subsequently informed with the empty holder's measured s-parameter. The effect of the sample holder on actual material measurement can be eliminated by using the de-embedding feature of the VNA. The outcomes from both approaches will be the same. The complex dielectric characteristics are then calculated from the measured s-parameters using a software. There are several ways for converting measured s-parameters into dielectric values which are included in a separate section below [6].

## 2.2 Open-ended coaxial probe method

A non-destructive testing technique for years has been the open-ended coaxial probe approach. As Fig. 3 represents, this technique measures the reflection coefficient and uses it to calculate the permittivity by pressing the probe against a sample or submerging it in the liquid [8]. Additionally, it might not be possible to cut out a sample of a material for some measurements. Because the material properties of biological specimens are susceptible to change, this is particularly crucial for in-vivo measurements. As a result, adopting this technique allows for intimate contact between the sample and probe without affecting the material's properties, however, for the purpose of this study these things do not matter as the main interest is the dielectric liquids that are used for the electric insulation equipment [9, 10].

An analysis tool for vector networks is used to measure the reflection coefficient. The VNA with a probe system is first calibrated so that the measurements of the reflection coefficient are in relation to the aperture plane of the probe. There are two ways to accomplish this. The first technique directly calibrates the probe's open end using reference liquids. It is incredibly clear and uncomplicated. However, the measurement's uncertainties are brought on by ambiguities in the choice of reference liquids and their characterization as calibration standards [11].

The standards (a short, an open, and a referenced liquid) are placed at the end of the probe to perform all measurements according to the procedure. Referenced liquids must have "known" dielectric characteristics in order to be utilized as calibration standards. The standard reference liquids are typically chosen to be water, saline, and methanol. Then, a standard one port full calibration is used. A program

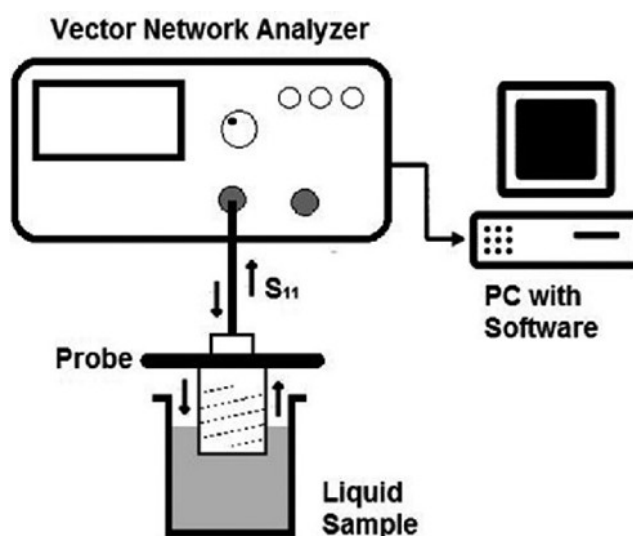


Fig. 3 Open-ended coaxial cable method measurement implementation

can be used to post-process the s-parameters measured on the MUT to derive the dielectric parameters [12, 13]. In the second method's measurement process the connection calibration plane is calibrated using standard calibration, and the probe aperture is translated using a simulated model of the probe. The reflection coefficient at the probe aperture is then used to calculate the permittivity. The accuracy of the measurement is closely correlated with the accuracy of the physical parameters of the probe's aperture [14, 15].

Using a calibration reference, the VNA is calibrated during the calibration procedure at the connector plane (open, short and match). The connector plane is then used to attach the probe. The reflections from the connector are reduced using the gating function of the time domain feature in the VNA. Two stages are taken during recording and post processing of the complex coefficient data  $\Gamma_c$  that is referenced to the connector plane. The measurement reference is moved from the connector plane to the probe aperture plane in the first stage using a model to correct the probe's propagation characteristics. The embedded reflection coefficient, denoted as  $\Gamma_a$ , will be derived by the model. The probe is handled as a two-port microwave network using the de-embedding model, and an equation is utilized to relate the reflection coefficient at the connection to the reflection coefficient at the aperture plane using s-parameters. The observed data  $\Gamma_c$  and the simulated data  $\Gamma_a$  are used to calculate the unknown s-parameters [3]. The reflection coefficients ( $\Gamma_c$ ) of three reference liquids or samples are measured for the measured data. With the aid of a simulation model of an ideal probe submerged in each of the reference liquids, the embedded reflection coefficient  $\Gamma_a$  was calculated. The data combinations allow for the determination of the s-parameter. The model can determine the unknown reflection coefficient  $\Gamma_a$  from the measurement reference plane reflection coefficients at  $\Gamma_c$  by determining the s-parameters [13]. The study employed a technique to determine the dielectric constant of a test material applied as the dielectric of a coaxial cable. The input impedance of the cable changes with frequency and relative permittivity, and the dielectric constant was calculated by analysing the reflected wave spectrum of a short-circuited coaxial line. To verify the accuracy of the results, the complex dielectric constant values obtained using this method were compared with those measured by other techniques. This novel measurement approach offers a means of exploring the dielectric characteristics of various materials.

### 3 Conversion methods

#### 3.1 Nichols-Ross-Weir method

The NRW technique relies on assessing the reflection and transmission of light through a uniform sample of isotropic material, following predetermined lighting conditions. The material has complex permittivity  $\epsilon(\omega) = \epsilon_r \epsilon_0(\omega) = \epsilon'(\omega) - \epsilon''(\omega)$  and permeability  $\mu(\omega) = \mu_r(\omega)\mu_0 = \mu'(\omega) - j\mu''(\omega)$  and occupies the region between the planes  $z = 0$  and  $z = d$ , while the regions  $z < 0$  and  $z > d$  are assumed to be free space. The sample receives illumination from a wave originating below  $z = 0$ . Three specific scenarios are considered. In the first scenario, the material is illuminated in a free space environment by either a parallel or perpendicular-polarized plane wave, which is angled at  $\theta_0$  from the normal to the material. Here, the material is assumed to extend infinitely in the x and y directions. In the second scenario, the material is situated within a guided wave structure operating in the TEM (Transverse Electromagnetic) mode, such as a coaxial cable or a stripline. It is assumed that the material completely fills the cross-section of the structure and only the TEM mode is present throughout. In the third scenario, the material occupies a guiding wave structure with either a single TE (Transverse Electric) or TM (Transverse Magnetic) mode present throughout all regions. The objective of the NRW method is to evaluate the permittivity ( $\epsilon$ ) and permeability ( $\mu$ ) by analyzing the reflection coefficient ( $S_{11}$ ) and the transmission coefficient ( $S_{21}$ ). These coefficients represent the ratio of the reflected or transmitted transverse electric field to the incident transverse electric field at the planes of the material sample [16]. The NRW method offers several advantages. It is characterized by its speed and non-iterative nature, making it efficient for analysis. Additionally, it can be applied effectively to both waveguides and coaxial lines, enhancing its versatility. However, there are limitations to consider. The method may experience divergence issues at frequencies corresponding to multiples of one-half wavelength, which could affect its accuracy in certain scenarios. Furthermore, it is recommended to use relatively short samples, and it may not be suitable for materials with low levels of loss.

#### 3.2 NIST iterative method

The NIST Iterative method employs the Newton-Raphson's root finding technique specifically for calculating permittivity. It utilizes either all four ( $S_{11}$ ,  $S_{21}$ ,  $S_{12}$ ,  $S_{22}$ ) or a pair

( $S_{11}$ ,  $S_{21}$ ) of s-parameters of the Material Under Test (MUT) to compute both reflection and transmission coefficients. This method performs effectively when an accurate initial guess is provided and bypasses the inaccuracies encountered in the NRW method, particularly when the sample thickness corresponds to an integer multiple of one-half wavelength ( $n\lambda/2$ ). It is particularly suitable for analyzing long samples and characterizing materials with low levels of loss [17]. However, without a precise initial guess, the solution may diverge or yield highly inaccurate results. Moreover, the NIST iterative method operates under the assumption that permeability equals unity, limiting its applicability to nonmagnetic materials exclusively [18].

### 3.3 NIST non-iterative method

The new non-iterative method bears resemblance to the NRW method but features a distinct formulation, particularly suitable for calculating permittivity when permeability is less than or equal to 1. It leverages either all four ( $S_{11}$ ,  $S_{21}$ ,  $S_{12}$ ,  $S_{22}$ ) or just two ( $S_{11}$ ,  $S_{21}$ ) s-parameters of the Material Under Test (MUT) to compute reflection and transmission coefficients. Notably, this method offers stability across a broad frequency range for samples of arbitrary length, a significant advantage. It is based on a simplified version of the NRW method, ensuring no divergence occurs at frequencies corresponding to multiples of one-half wavelength in the sample. Unlike some methods, it doesn't require an initial estimation of permittivity, enabling swift calculations. Despite its non-iterative nature, its accuracy rivals that of iterative methods. Moreover, this method features a partly different formulation from the NRW method and can be easily extended to other sample types, such as micro-strip or coplanar lines. Additionally, the expressions derived from this method include both permittivity and permeability, providing insights into the effective electromagnetic parameters representing a propagation mode. The new non-iterative method presents several advantages. Firstly, it yields smooth permittivity results without encountering divergence, ensuring reliability. Secondly, it boasts accuracy in its calculations. Thirdly, it accommodates samples of arbitrary length, enhancing its versatility. Additionally, it operates swiftly and non-iteratively, contributing to efficiency. Importantly, it eliminates the need for an initial guess in the calculation process. However, like the NIST iterative method, it is applicable solely for permittivity measurement, which could be considered a limitation [17].

### 3.4 The Short-Circuit Line method

The SCL method involves placing a sample within a section of rectangular waveguide and measuring the  $S_{11}$ -parameter while the waveguide is terminated by two offset shorts of different lengths [19]. These S-parameter measurements are utilized to determine the input impedance of the sample under various conditions. Using these input impedances alongside transmission-line equations, the complex permittivity and permeability of the sample can be extracted across the frequency range of interest. However, for this method to be effective, the thickness of the material sample must be less than one-half wavelength to prevent the excitation of higher order modes, particularly the TE<sub>10</sub> mode, within the sample. The possibility of higher mode excitation arises due to slight imperfections in the machining of the samples, which may not perfectly match the waveguide geometry, leading to inhomogeneities within the sample. This can result in a loss of orthogonality between the modes of the empty waveguide and those within the sample region. Additionally, another constraint on the sample thickness arises from the need for low-loss samples to be thick enough to yield significant reflections. Failure to meet both of these thickness conditions can lead to the generation of erroneous data for the extracted values of permittivity and permeability, particularly at high frequencies. Further details on this method can be found in the referenced literature [20].

## 4 Equipment

The experiment involved the use of various tools, including a VNA, specifically the LiteVNA 64. The VNA is a portable device capable of measuring reflection and transmission coefficients across a wide frequency range (50 kHz to 6.3 GHz). The LiteVNA, modelled after the NanoVNA and SAA2, employs a single mixer for  $S_{11}$  and  $S_{21}$  measurements by switching the radio frequency and performing IFFT calculations for TDR/DTF measurements. The LiteVNA eliminates the need for a large analyser, making it a convenient tool for equipment testing and measurement. To connect the VNA to the test material, a  $2 \times 30$  cm SMA MALE-MALE SS405 RF coaxial cable and SMA to N type connector were used. The test material was held in a bespoke (150 mm) 3D printed hollow cylinder Electrifi Conductive Filament with outer and inner diameters of both (20 mm) and (2.00 mm), respectively, with an N type female inlet. For accurate readings, the VNA required calibration, which involved three calibration steps: short circuit, open circuit, and load calibration using the connectors that come with the device for this purpose.

### 5 Tested samples

Palm oil, sunflower oil, and rapeseed oil; the samples which were tested in this study are all vegetable oils with different chemical compositions and physical properties as shown in Table 1.

Palm oil, derived from the fruit of oil palm trees, is a semi-solid vegetable oil with a notable saturated fat content. It finds applications in food products, cosmetics, and biofuels. However, its susceptibility to oxidation can result in the production of harmful by-products and deterioration of its properties over time [21]. Conversely, sunflower oil, a liquid vegetable oil obtained from sunflower seeds, possesses low levels of saturated fats and is rich in polyunsaturated fats. It exhibits superior resistance to aging compared to mineral oil, making it a potential substitute for electrical insulation purposes [22]. Rapeseed oil, also known as canola oil, is a vegetable oil extracted from rapeseed plants' seeds. It is low in saturated fats but high in both monounsaturated and polyunsaturated fats. The exceptional heat capacity and thermal stability of rapeseed oil make it a promising candidate for thermal energy storage applications, specifically as a phase change material [23]. The properties of these oils can be influenced by factors such as the presence of antioxidants, the incorporation of nanoparticles, and the blending with other oils [24]. Samples are typically subjected to measurements under standard ambient humidity conditions, which commonly range from 40% to 60% relative humidity. However, when dealing with liquid samples, the humidity of the sample holder becomes a critical factor due to their high sensitivity to moisture. Therefore, meticulous attention was given to maintaining a completely dry state for the sample holder to ensure optimal contact between the samples and the sample holder walls. This strict requirement aimed to prevent any alteration of the original physical parameters of the samples, including temperature and humidity.

**Table 1** Physical properties of the samples used in the test

Oil Type	Density at 20 °C Kg/dm <sup>3</sup>	Fire Point °C	Break-down (V)	Viscosity at 90 °C	Specific Heat at 20 °C
Palm Oil	0.92	345	50	32.5	320
Sunflower Oil	0.919	>365	>60	41	>330
Rapeseed Oil	0.9	340	>45	43.5	325

### 6 Analysis

Upon connecting the sample holder to the 11 port of the VNA, the reflected waveform of the impedance value for each tuned frequency is displayed on the VNA screen. The complex permittivity for each frequency and its corresponding input impedance value can be measured based on this. This is accomplished by utilizing the formula for the short circuit finite coaxial cable below:

$$Z_{IN} = i Z_o \tan \beta l \tag{8}$$

$Z_{IN}$ : Input impedance ( $\Omega$ ).

$\beta$ : Phase constant (rad/m).

$l$ : Length of the sample holder (m).

The characteristic impedance of the coaxial line can be expressed as a function of the relative permittivity, as demonstrated below:

$$Z_o = \frac{138}{\sqrt{\epsilon_r}} \log \frac{D_1}{D_2} \tag{9}$$

$\epsilon_r$ : Complex dielectric permittivity.

$D_1$ : Outer diameter of the test sample (m).

$D_2$ : Inner diameter of the sample holder (m).

The phase constant is dependent on the relative permittivity and can be computed using the following equation:

$$\beta = 2\pi \frac{f}{c} \sqrt{\epsilon_r} \tag{10}$$

$f$ : Frequency of the reflected wave (Hz).

$c$ : Speed of light (m/s).

Thus, the reflected signal on the  $S_{11}$  also can be written as:

$$Z_{IN} = i \frac{138}{\sqrt{\epsilon_r}} \log \left( \frac{D_1}{D_2} \right) \tan 2\pi \frac{f}{c} \sqrt{\epsilon_r} l \tag{11}$$

### 7 Results

The given complex equation for input impedance, complex permittivity, and frequency does not provide direct values that can be evaluated. To obtain exact values for the permittivity, the Newton Raphson method was employed, using iterations and initial guesses. Among the possible solutions obtained, there is only one that is consistently meaningful for the complex permittivity. Experimental measurements of the input impedance for various oil samples were conducted at frequencies ranging from 1 MHz to 10 MHz. Despite this relatively narrow frequency band used to study

the complex dielectric permittivity, it was sufficient to give a good indication about the effectiveness reliability of this method which is one of the goals of this study. It was observed that the real part of the permittivity for all oil samples exhibited a decreasing trend as the input frequency increased. This behaviour was expected and depicted in Fig. 4, with a sharp decline observed when approaching frequencies close to 10 MHz. It is important to note that all measurements were performed at a sample temperature of approximately 25 °C. Regarding the dielectric loss, as represented in Fig. 5, a distinct behaviour is observed. Palm Oil and Rapeseed Oil exhibit a minor increase in dielectric loss with increasing frequency, which is discernible up to 10 MHz. On the other hand, Sunflower Oil demonstrates an inversely proportional relationship between dielectric loss and frequency, starting at a higher frequency compared

to the other samples tested. It is important to note that the measurements were conducted at a sample temperature of 25 °C. Previous studies were conducted to evaluate the dielectric properties of frying Palm Oil had similar findings in terms of the dielectric constant and losses under mutual frequency values, an impedance analyser was used to apply a certain voltage at variable frequency settings to calculate the input impedance followed by the dielectric permittivity [25, 26]. As for the Sunflower Oil and Rapeseed Oil, same results were found for both complex permittivity values for the same frequency sets where a similar approach was adopted for the reflection coefficient. But the numerical calculations were performed using the Cole-Cole model in [27]. Meanwhile a parallel plate method to measure the capacitance is deployed in [28].

### 8 Discussion

The discussion focuses on the proposed Short Circuit Line method as a reliable alternative for assessing the dielectric properties of liquids. The method has its own advantages, including smooth results without divergence, high accuracy, and flexibility in sample length. Moreover, the method enables the measurement of various properties of the test sample beyond just permittivity, such as capacitance and characteristic impedance. The compact size of the tools used in this method makes them practical for implementation in diverse work environments. Additionally, the minimal sample volume required for testing ensures a "non-destructive" nature, which is particularly beneficial for operational devices like power transformers.

Future investigations could focus on enhancing the precision of the instruments, reducing the margin of error, and establishing regular utilization of the method. Moreover, exploring the effectiveness of this method at different temperatures and expanding the tested frequency range to the UHF spectrum could provide valuable insights into the behaviour of dielectric permittivity under varying conditions.

### 9 Conclusion

The proposed Short Circuit Line method offers a promising alternative for assessing the dielectric properties of liquids with medium to high loss. Its advantages, including smooth results, high accuracy, and flexibility in sample length, make it a valuable tool for researchers and practitioners in various fields. Furthermore, the method's non-destructive nature, compact size, and ability to measure multiple properties of the test sample contribute to its practicality and usability in

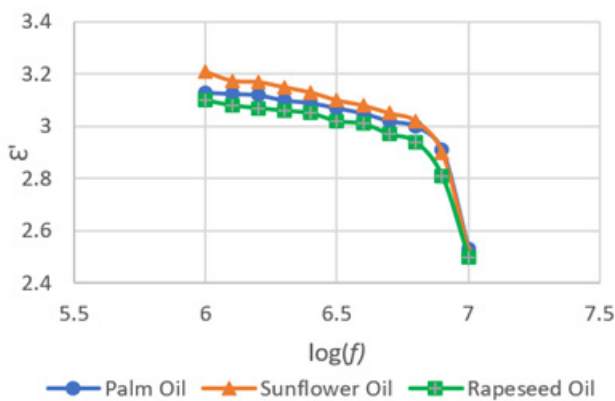


Fig. 4 Dielectric permittivity (Real Permittivity) for Palm, Sunflower, and Rapeseed oils with respect to the input frequency through the samples at 25 °C.

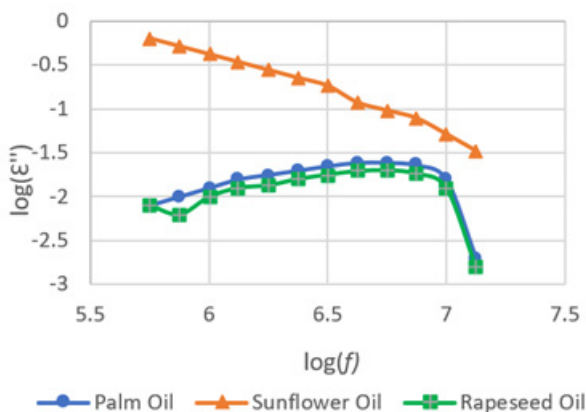


Fig. 5 Dielectric loss (Imaginary Permittivity) for Palm, Sunflower, and Rapeseed oils with respect to the input frequency through the samples at 25 °C.

diverse applications. Future research efforts aimed at refining the instruments, exploring different environmental conditions, and expanding the frequency range could further enhance the method's utility and effectiveness.

## References

- [1] Boughriet, A.-H., Legrand, C., Chapoton, A. "Noniterative stable transmission/reflection method for low-loss material complex permittivity determination", *IEEE Transactions on Microwave Theory and Techniques*, 45(1), pp. 52–57, 1997.  
<https://doi.org/10.1109/22.552032>
- [2] Baker-Jarvis, J. "Transmission/reflection and short-circuit line permittivity measurements", National Institute of Standards and Technology, Washington, USA, (Technical Note 1341) 1990.
- [3] Popovic, D., McCartney, L., Beasley, C., Lazebnik, M., Okoniewski, M., Hagness, S. C., Booske, J. H. "Precision open-ended coaxial probes for in vivo and ex vivo dielectric spectroscopy of biological tissues at microwave frequencies", *IEEE Transactions on Microwave Theory and Techniques*, 53(5), pp. 1713–1722, 2005.  
<https://doi.org/10.1109/TMTT.2005.847111>
- [4] Baker-Jarvis, J., Vanzura, E. J., Kissick, W. A. "Improved technique for determining complex permittivity with the transmission/reflection method", *IEEE Transactions on Microwave Theory and Techniques* 38(8), pp. 1096–1103, 1990.  
<https://doi.org/10.1109/22.57336>
- [5] Folgerø, K. "Bilinear calibration of coaxial transmission/reflection cells for permittivity measurement of low-loss liquids", *Measurement Science and Technology*, 7(9), 1260, 1996.  
<https://doi.org/10.1088/0957-0233/7/9/011>
- [6] Baek, K.-H., Sung, H.-Y., Park, W. S. "A 3-position transmission/reflection method for measuring the permittivity of low loss materials", *IEEE Microwave and Guided Wave Letters*, 5(1), pp. 3–5, 1995.  
<https://doi.org/10.1109/75.382378>
- [7] Shenhui, J., Ding, D., Quanxing, J. "Measurement of electromagnetic properties of materials using transmission/reflection method in coaxial line", In: *Asia-Pacific Conference on Environmental Electromagnetics*, Hangzhou, China, 2003, pp. 590–595. ISBN 7-5635-0802-3  
<https://doi.org/10.1109/CEEM.2003.238488>
- [8] Burdette, E. C., Cain, F. L., Seals, J. "In Vivo Probe Measurement Technique for Determining Dielectric Properties at VHF through Microwave Frequencies", *IEEE Transactions on Microwave Theory and Techniques*, 28(4), pp. 414–427, 1980.  
<https://doi.org/10.1109/TMTT.1980.1130087>
- [9] Gabriel, S., Lau, R. W., Gabriel, C. "The dielectric properties of biological tissues: II. Measurements in the frequency range 10 Hz to 20 GHz", *Physics in Medicine & Biology*, 41, 2251, 1996.  
<https://doi.org/10.1088/0031-9155/41/11/002>
- [10] Peyman, A., Holden, S., Gabriel, C. "Mobile telecommunications and health research programme: Dielectric properties of tissues at microwave frequencies", Health Protection Agency Centre for Radiation Chemical and Environmental Hazards, 2005.
- [11] Wang, Z., Kelly, M. A., Shen, Z.-X., Wang, G., Xiang, X.-D., Wetzel, J. T. "Evanescent microwave probe measurement of low- $k$  dielectric films", *Journal of Applied Physics*, 92(2), pp. 808–811, 2002.  
<https://doi.org/10.1063/1.1481199>
- [12] Chew, W. C., Olp, K. J., Otto, G. P. "Design and calibration of a large broadband dielectric measurement cell", *IEEE Transactions on Geoscience and Remote Sensing*, 29(1), pp. 42–47, 1991.  
<https://doi.org/10.1109/36.103291>
- [13] Nyshadham, A., Sibbald, C. L., Stuchly, S. S. "Permittivity measurements using open-ended sensors and reference liquid calibration—an uncertainty analysis", *IEEE Transactions on Microwave Theory and Techniques*, 40(2), pp. 305–314, 1992.  
<https://doi.org/10.1109/22.120103>
- [14] Gregory, A. P., Clarke, R. N. "A review of RF and microwave techniques for dielectric measurements on polar liquids", *IEEE Transactions on Dielectrics and Electrical Insulation*, 13(4), pp. 727–743, 2006.  
<https://doi.org/10.1109/TDEI.2006.1667730>
- [15] H. Packard "Automating the HP 8410B microwave network analyzer", Hewlett Packard, pp. 1–25, 1980. [online] Available at: [https://www.hpmemoryproject.org/an/pdf/an\\_221a.pdf](https://www.hpmemoryproject.org/an/pdf/an_221a.pdf) [Accessed: 24 May 2023]
- [16] Rothwell, E. J., Frasch, J. L., Ellison, S. M., Chahal, P., Ouedraogo, R. O. "Analysis of the Nicolson-Ross-Weir Method for Characterizing the Electromagnetic Properties of Engineered Materials", *Progress In Electromagnetics Research*, 157, pp. 31–47, 2016.  
<https://doi.org/10.2528/PIER16071706>
- [17] Yaw, K. C. "Measurement of dielectric material properties", Rohde & Schwarz, 2012. [online] Available at: [https://cdn.rohde-schwarz.com/pws/dl\\_downloads/dl\\_application/00aps\\_undefined/RAC-0607-0019\\_1\\_5E.pdf](https://cdn.rohde-schwarz.com/pws/dl_downloads/dl_application/00aps_undefined/RAC-0607-0019_1_5E.pdf) [Accessed: 23 May 2023]
- [18] Baker-Jarvis, J., Janezic, M. D., Riddle, B. F., Johnk, R. T., Kabos, P., Holloway, C. L., Geyer, R. G., Grosvenor, C. A. "Measuring the permittivity and permeability of lossy materials: Solids, liquids, metals, building materials, and negative-index materials", National Institute of Standards and Technology, USA, NIST Technical Note 1536, 2005.
- [19] Wolfson, B. J., Wentworth, S. M. "Complex permittivity and permeability measurement using a rectangular waveguide", *Microwave and Optical Technology Letters*, 27(3), pp. 180–182, 2000.  
[https://doi.org/10.1002/1098-2760\(20001105\)27:3<180::AID-MOP9>3.0.CO;2-D](https://doi.org/10.1002/1098-2760(20001105)27:3<180::AID-MOP9>3.0.CO;2-D)
- [20] Wolfson, B. J., Wentworth, S. M. "Complex permittivity and permeability measurement at elevated temperatures using rectangular waveguide", *Microwave and Optical Technology Letters*, 38(6), pp. 449–453, 2003.  
<https://doi.org/10.1002/mop.11086>



- [21] Rao, U. M., Sood, Y. R., Jarial, R. K. "Oxidation stability enhancement of a blend of mineral and synthetic ester oils", *IEEE Electrical Insulation Magazine* 32(2), pp. 43–47, 2016.  
<https://doi.org/10.1109/MEI.2016.7414230>
- [22] Singha, S., Asano, R., Frimpong, G., Claiborne, C. C., Cherry, D. "Comparative aging characteristics between a high oleic natural ester dielectric liquid and mineral oil", *IEEE Transactions on Dielectrics and Electrical Insulation*, 21(1), pp. 149–158, 2014.  
<https://doi.org/10.1109/TDEI.2013.003713>
- [23] Pasupathi, M. K., Alagar, K., Matheswaran, M. M., Aritra, G. "Characterization of Hybrid-nano/Paraffin Organic Phase Change Material for Thermal Energy Storage Applications in Solar Thermal Systems", *Thermal Energy Storage in Building Integrated Thermal Systems*, 13(19), 5079, 2020.  
<https://doi.org/10.3390/en13195079>
- [24] Madavan, R. Balaraman, S. "Comparison of antioxidant influence on mineral oil and natural ester properties under accelerated aging conditions", *IEEE Transactions on Dielectrics and Electrical Insulation*, 24(5), pp. 2800–2808, 2017.  
<https://doi.org/10.1109/TDEI.2017.006527>
- [25] Pecovska-Gjorgjevich, M., Andonovski, A., Velevska, J. "Measuring frequency-and temperature-dependent permittivities of vegetable oils", *Physica Macedonica*, 59, pp. 77–89, 2010.
- [26] Ibrahim, N. U. A., Abd Aziz, S., Hashim, N., Jamaludin, D., Khaled, A. Y. "Dielectric Spectroscopy of Palm Olein During Batch Deep Frying and Their Relation with Degradation Parameters", *Journal Food Science*, 84(4), pp. 792–797, 2019.  
<https://doi.org/10.1111/1750-3841.14436>
- [27] Vrba, J. Vrba, D. "Temperature and Frequency Dependent Empirical Models of Dielectric Properties of Sunflower and Olive Oil", *Radioengineering*, 22(4), pp. 1281–1287, 2013. [online] Available at: [https://www.radioeng.cz/full-texts/2013/13\\_04\\_1281\\_1287.pdf](https://www.radioeng.cz/full-texts/2013/13_04_1281_1287.pdf) [Accessed: 23 May 2023]
- [28] Lizhi, H., Toyoda, K., Ihara, I. "Dielectric properties of edible oils and fatty acids as a function of frequency, temperature, moisture and composition", *Journal of Food Engineering*, 88(2), pp. 151–158, 2008.  
<https://doi.org/10.1016/j.jfoodeng.2007.12.035>